



Full length article

## Fabrication of ZnO nanoparticles modified sensor for electrochemical oxidation of methdilazine



Nagaraj P. Shetti<sup>a,\*</sup>, Shweta J. Malode<sup>a</sup>, Deepti S. Nayak<sup>a</sup>, Gangadhar B. Bagihalli<sup>a</sup>, Shankara S. Kalanur<sup>b</sup>, Ramesh S. Malladi<sup>c</sup>, Ch. Venkata Reddy<sup>d</sup>, Tejraj M. Aminabhavi<sup>e</sup>, Kakarla Raghava Reddy<sup>f,\*</sup>

<sup>a</sup> Electrochemistry and Materials Group, Department of Chemistry, K.L.E. Institute of Technology, Gokul, Hubballi 580030, Affiliated to Visvesvaraya Technological University, Karnataka, India

<sup>b</sup> Department of Materials Science and Engineering, Ajou University, Suwon 443-739, Republic of Korea

<sup>c</sup> Department of Chemistry, BLDEA's V. P. Dr. P. G. Halakatti College of Engineering and Technology, Vijayapur 586103, Karnataka, India

<sup>d</sup> School of Mechanical Engineering, Yeungnam University, Gyeongsan 712-749, South Korea

<sup>e</sup> Soniya College of Pharmacy, Dharwad, Karnataka, India

<sup>f</sup> School of Chemical and Biomolecular Engineering, The University of Sydney, Sydney, NSW 2006, Australia

## ARTICLE INFO

## Keywords:

Metal oxide nanoparticles  
Surface properties  
Electrochemistry  
Electrocatalytic behavior  
Glassy carbon electrode  
Heterogeneous rate constant  
Methdilazine

## ABSTRACT

In recent years, semiconductor nanostructures have gained enormous attention of researchers because of their excellent electrocatalytic activity and applications in various fields. Zinc oxide (ZnO) nanoparticles, which possess excellent electrocatalytic properties and stability, are versatile materials for a variety of sensing applications. The present research presents the fabrication of the ZnO-nanoparticle-modified glassy carbon electrode and its application to quantify an antihistamine drug, methdilazine (MDH). Transmission electron microscopy, and X-ray diffraction studies were carried out to investigate the surface characteristics of ZnO nanoparticles. Furthermore, to investigate the effects of pH, accumulation time, scan rate, excipients, and concentration on the oxidation behavior of MDH, cyclic voltammetry, linear sweep voltammetry, and square wave voltammetry were carried out at a pH of 10.4. The electrode displayed excellent analytical performance for the quantification of MDH with a low limit of detection compared to earlier reports. The constructed sensor showed outstanding characteristics and could be readily applied to analyze MDH in urine and pharmaceutical samples.

## 1. Introduction

One of the biggest challenges of present-day surface science is to identify efficient modifiers for electrodes to detect drug molecules selectively. Modifiers with low electrical conductivity, high surface area, long-lasting stability, cost effectiveness, and high porosity have gained the attention of researchers [1–3]. Interestingly, the above characteristics are realized in semiconductor nanoparticles. In recent years, semiconductor nanoparticles have been of immense interest to researchers due to their application potential in the field of material science, electrical and chemical engineering [4–7].

ZnO nanoparticles have a wurtzite structure with a large surface area that makes it a useful material in the field of biosensors. It has a large band gap of 3.37 eV, and a high exciton binding energy of 60 MeV, at ambient temperature. The ZnO nanoparticle possesses chemical and physical properties different from those of bulk ZnO.

Applications of ZnO nanoparticles have been extended to fields such as electro and photoluminescent materials [8], gas sensors [9], ultraviolet nanolasers [10], optical modulator waveguides [11], and solar cells [12]. The powdered form of ZnO exhibits good electrical conductivity and optical transmission. Additionally, these are low-priced and non-hazardous. Moreover, Zn and O atoms in ZnO nanoparticles have a large difference in the irrespective electronegativities, making the bonding extremely ionic. As oxide semiconductors strong adsorption and catalytic abilities, they are applicable in a variety of sensors such as gas sensors, electrochemical sensors as well as biosensors, and environmental applications [13,14]. These attractive features of ZnO nanoparticles prompted us to develop zinc oxide modified glassy carbon electrode (ZnO-GCE) for the detection as well as to understand the degradation products of MDH.

In this study, a glassy carbon electrode (GCE) was selected as a stable base to fabricate a ZnO-nanoparticle-modified glassy carbon

\* Corresponding authors.

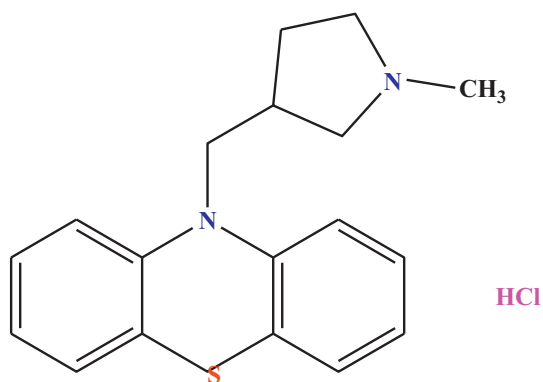
E-mail addresses: [dr.npshetti@gmail.com](mailto:dr.npshetti@gmail.com) (N.P. Shetti), [reddy.chem@gmail.com](mailto:reddy.chem@gmail.com) (K.R. Reddy).

<https://doi.org/10.1016/j.apsusc.2019.143656>

Received 18 February 2019; Received in revised form 21 July 2019; Accepted 11 August 2019

Available online 12 August 2019

0169-4332/ © 2019 Elsevier B.V. All rights reserved.



**Scheme 1.** Chemical structure of Methdilazine hydrochloride (MDH).

electrode (ZnO-GCE). Since the past decade, GCEs have been widely used by researchers in the field of modified sensors because of their vast applicable potential window, small residual background current, reproducibility of successive voltammetric scans, good stability, low cost, and quick surface renewal after the usage with diverse sorts of modulators [15,16].

Methdilazine hydrochloride (MDH) (Scheme 1) is a common anti-histamine drug, which also shows anti-pyretic behavior. It is a synthetic derivative of phenothizone, chemically known as 10-[(1-Methyl-3 pyrrolidinyl) methyl] phenothiazine monohydrochloride [17].

Recently, a few techniques for the analysis of MDH in pharmaceuticals have been found, such as liquid chromatography [18], high-performance liquid chromatography, reversed-phase and ion-exchange electro chromatography [19,20], spectrofluorimetry [21], differential UV-spectrophotometry and differential fluorimetry [22], and visible spectrophotometric methods [23]. Though these reported methods are well established, they have drawbacks such as elaborate sample preparation, costly equipment, long analysis time, and the need for specialized expertise. On the other hand, the electrochemical methods have proved to be the best technique for the quantification of any molecules because of their easy sample preparation, relatively less expensive equipment, quick response time, and accuracy. However, only one electrochemical method has been reported for the analysis of MDH with glassy carbon as the working electrode, which uses cyclic voltammetry (CV) and differential pulse voltammetry [24].

However, there is limited literature available for the estimation of MDH and the use of ZnO as an electrode material for sensor applications in the detection of bioactive compounds. In view of this, we report for the first time the usage of the ZnO-GCE as an efficient electrode material for the detection and electrooxidation studies of MDH. The electrochemical behavior of MDH was studied by CV, linear sweep voltammetry (LSV), and square wave voltammetry (SWV) techniques. The ZnO-GCE sensor was applied for the analysis of samples such as pharmaceutical dosage forms and human urine samples. We observed good recovery and low detection limit compared to other reported methods. This suggests that our electrode would be suitable as an alternative for quality control and clinical trials.

## 2. Experimental

### 2.1. Instrumentation and chemicals

Electrochemical measurements were performed on a potentiostat (D-630 electrochemical analyzer, USA). Three electrodes connected to the device were dipped into the test solution taken in a 10 mL single compartment cell. Platinum wire was used as the counter electrode, Ag/AgCl as the reference, and the ZnO-GCE as the working electrode.

MDH in its pure form was purchased from Sigma-Aldrich and its stock solution (1.0 mM) was prepared in double distilled water. It was

stored in a cold and dark place until used. The phosphate buffer saline (PBS) solution with a pH range from 3.0 to 11.2 [25], having an ionic strength of 0.2 M, was used as the supporting electrolyte. Analytical grade reagents and double distilled water were used throughout the experiments.

### 2.2. Synthesis of ZnO nanoparticles

In a typical procedure for synthesis of ZnO nanoparticles, 0.2 mol of zinc acetate [ $\text{Zn}(\text{CH}_3\text{COO})_2 \cdot 2\text{H}_2\text{O}$ ] in 50 mL of solvent (equal volume of deionized water and ethanol), and an equal molar amount of sodium hydroxide in another deionized water–ethanol matrix were mixed drop by drop. The reaction mixture was stirred for 4 h magnetically at 80 °C until a homogeneous white solution was obtained. Then, it was thoroughly washed with deionized water and ethanol, and the solution was centrifuged at 10,000 rpm about 30 min. The settled powder was collected and dried in a hot air oven at 120 °C for 2 h to get ZnO powder. The final product was calcinated at 550 °C at different time such as 3, 7 and 12 h.

### 2.3. Pretreatment of the glassy carbon electrode

Initially, the surface of a bare GCE was carefully polished with 3.0  $\mu\text{m}$  alumina powder using micro cloth pads and then thoroughly rinsed with double distilled water until a shining surface was obtained. Any impurity present on the surface of the working electrode can interfere with voltammetric signals to give inaccurate results. Hence, this careful procedure was carried out to clean the surface of the electrode [26].

### 2.4. Preparation of modified electrode

A white suspension of ZnO nanoparticles was prepared by dispersing approximately 1 mg of ZnO nanoparticles in 10 mL ethanol using an ultrasonicator. Before each CV measurement, the GCE was polished carefully with  $\text{Al}_2\text{O}_3$  (0.3  $\mu\text{m}$ ) using a muslin cloth, followed by rinsing with ethanol and double distilled water to eliminate the  $\text{Al}_2\text{O}_3$  particles settled on the surface. The cleaned GCE was coated with 10  $\mu\text{L}$  of nano ZnO suspension and dried. The modified GCE was then functionalized in a buffer solution of pH 10.4 by performing a CV scan in the working potential range till a stable CV signal was found. Finally, the pretreated electrode was transferred to a 10 mL glass cell containing the buffer solution of pH 10.4 and the analyte.

### 2.5. Procedures for pharmaceutical preparations and spiked human urine samples

MDH containing the ‘Dilosyn’ syrup (5 mL = 4 mg MDH) was purchased from local commercial sources. A portion of this product, equivalent to the stock solution of MDH, was calculated, dissolved, and prepared in double distilled water. The proper amount of this solution was analyzed using SWV under optimum conditions. The quantity of MDH in the syrup sample was determined by using a calibration graph. Likewise, the effect of excipients was also studied to check the accuracy of the proposed method.

Drug-free urine samples collected from five healthy volunteers were filtered and stored frozen before usage. The samples were diluted 100 times with a phosphate buffer solution of pH 10.4. The urine samples were then spiked with standard MDH solution. The SWV technique was used under the optimum experimental conditions for the preparation of the calibration plot. Five replicates of samples were analyzed to examine the accuracy and precision of the proposed method.

### 3. Results and discussion

#### 3.1. Active surface area of the modified electrode

The surface vicinity of the modified electrode was calculated by the Randles–Sevcik equation. The CV technique was carried out at different sweep rates at 25 °C [27] by using KCl (0.1 M) and  $K_3[Fe(CN)_6]$  (1.0 mM) solutions. We found an area of 0.04 cm<sup>2</sup> for the bare GCE, whereas for the modified electrode, this area was two times larger, i.e., 0.082 cm<sup>2</sup>.

$$I_p = (2.69 \times 10^5) n^{3/2} A_0 D_R^{1/2} \nu^{1/2} C_0^* \quad (1)$$

where  $n$  is the number of electrons involved in the reaction, i.e., (1),  $A_0$  is the surface area of the sensing base,  $D_R$  is the diffusion coefficient ( $7.6 \times 10^{-6}$  cm<sup>2</sup> s<sup>-1</sup>) in the current procedure,  $\nu$  is the scan rate, and  $C_0^*$  is the concentration of  $K_3[Fe(CN)_6]$  (1.0 mM).

#### 3.2. Characterization of ZnO nanoparticles

Transmission electron microscopy (TEM) and X-ray Diffraction (XRD) analysis were performed to investigate the surface characteristics of ZnO nanoparticles (Fig. 1). Fig. 1 (a, b and c) shows the TEM images of ZnO nanoparticles prepared at 550 °C at different calcination time: a) 3, b) 7, and c) 12 h. It was found that the average crystallite sizes of ZnO nanoparticles prepared using different calcination time of 3, 7 and 12 h were 80, 55 and 20 nm, indicating the crystallite sizes of particles were decreased with increasing the calcination time. It is due to the calcination process can change the surface characteristics of ZnO particles, and close packing of particles without voids in the structure. The ZnO particles prepared at different calcination time were further analyzed

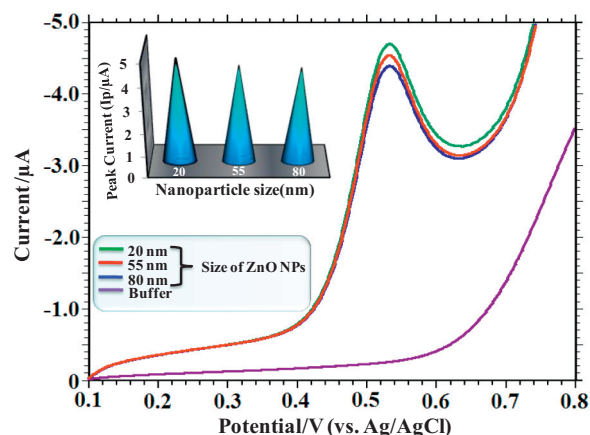


Fig. 2. Effect of size of ZnO nanoparticles on MDH electro-oxidation.

using XRD to determine their crystalline characteristics. As shown in Fig. 1d (i-iii), XRD pattern confirmed that all prepared ZnO samples have good crystalline nature and it is in accordance with JCPDS data (36-1451). The ( $h k l$ ) values of ZnO particles were labelled accordingly: (100), (002), (101), (102), (110), (103), (200), (112), (201), (004) and (202). XRD results reveal that no impurities were found in the diffraction pattern, suggesting that synthesized ZnO nanoparticles have an excellent purity. Using Scherrer's formula, the average crystal size was calculated and was found to be in the range of ~84 nm, 57 and 23 nm for ZnO nanoparticles prepared at calcination time of 3, 7 and 12 h.

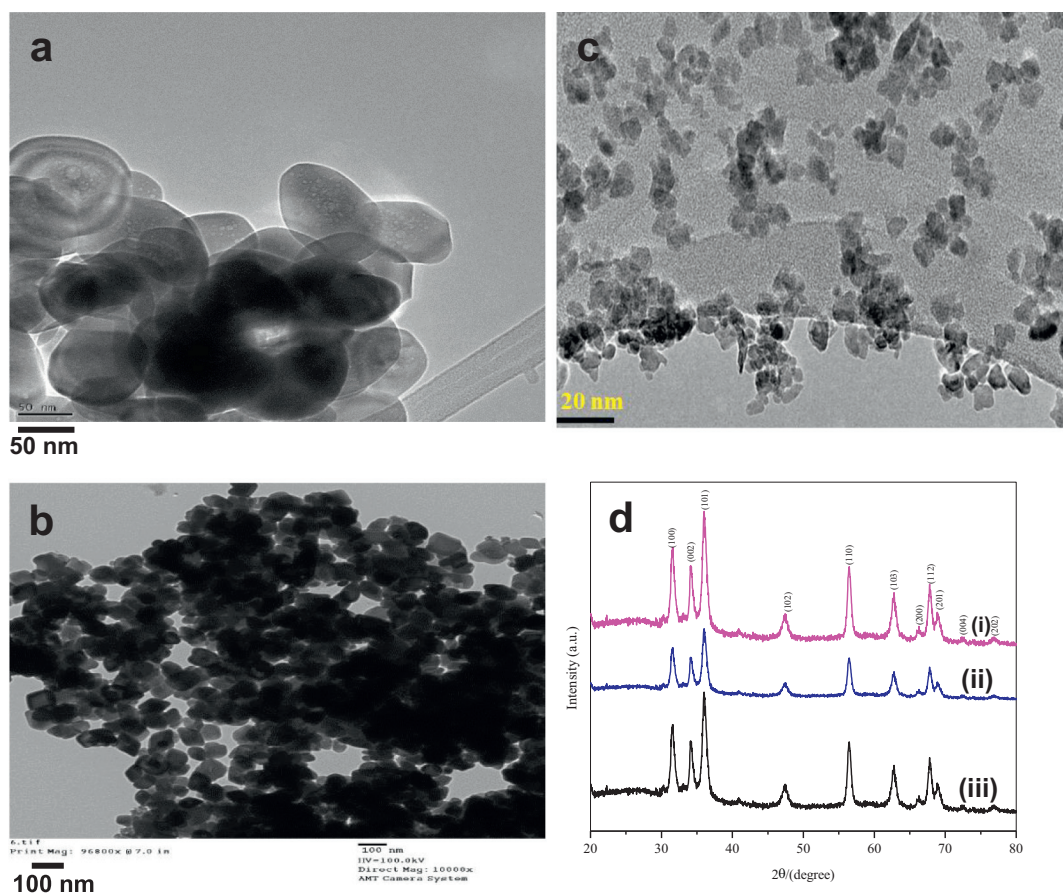


Fig. 1. TEM images of ZnO nanoparticles prepared at 550 °C in different calcination time: a) 3, b) 7, and c) 12 h. And d) XRD pattern of ZnO nanoparticles prepared at 550 °C in different calcination time: i) 3, ii) 7, and iii) 12 h.



### 3.3. Effect of size of ZnO nanoparticles

The effect of size of NPs was performed to confirm the size of ZnO on the electrode surface for further reaction and to verify if smaller size of them could be better adsorbed than larger particles. Fig. 2 shows the linear sweep voltammograms (LSVs) of MDH recorded using a same concentration but different sizes of ZnO nanoparticles ranging between 20 nm to 80 nm. It can be seen from figure that the electrode oxidation current was higher for 20 nm than the other size ZnO nanoparticles. This is due to the smaller the size of ZnO nanoparticles which results in the larger standard electrode potential. The ZnO modified sensor has higher standard electrode potential as it possess high surface energy leading to electrical energy to take part in the electrode reaction. The enhancement in the peak current by the average size of ZnO i.e., 20 nm takes place first than the bigger particles. Hence, further electrode parameters were studied using 20 nm sized ZnO.

### 3.4. Influence of ZnO nanoparticles amount to fabricate ZnO-GCE

The amount of modifier added influences the performance of the electrode as well as the electrochemical behavior of the analyte. Previous reports show that the addition of ZnO nanoparticles improves the electrochemical behavior because nanoparticles show signs of elevated catalytic activity per gram compared to bulk materials [14,28–30]. The nano sized ZnO is well known as a biomaterial for bio sensing and low cost. ZnO can be utilized to immobilize various biomolecules, since these show high catalytic efficiency, high isoelectric point of about 9.5, and strong adsorption capability, which are needed for adsorption of enzymes and antibodies by electrostatic interaction having low isoelectric point [29]. The ZnO nanoparticles help for the direct transfer of electrons between the sensing base and active sites of biomolecules. Moreover, the biocompatible nature of ZnO makes them to consider for various transduction techniques including piezoelectric, electrochemical, and optical and field effect transistor based detection.

In subsection 2.3, the preparation of the ZnO-GCE was described stepwise. The voltammograms of MDH and changes in the peak potential as well as in peak currents were recorded by varying the concentration of ZnO nanoparticles on the GCE. From the observations of peak potentials and currents, it was seen that a 0.5  $\mu\text{L}$  nano ZnO suspension was found to be optimal in modifying the GCE (Fig. 3).

### 3.5. Influence of pre-concentration time

Pre-concentration time influences the electrochemical activity of the drug by improving its peak intensity and sensitivity. Thus, to monitor this effect, pre-concentration time was studied in the range of 0–120 s.

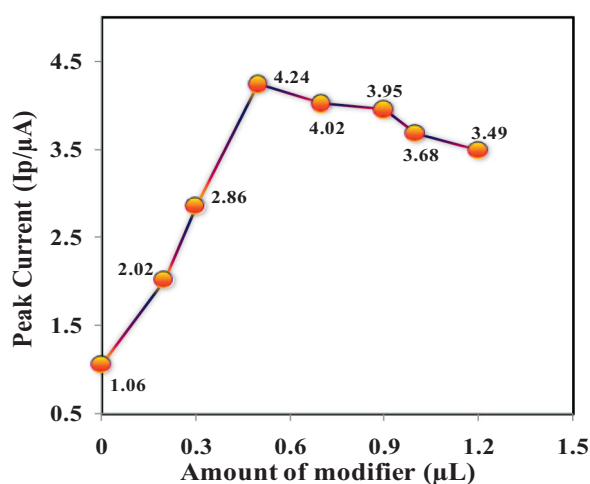


Fig. 3. Influence of ZnO nanoparticles amount on the peak current of MDH.

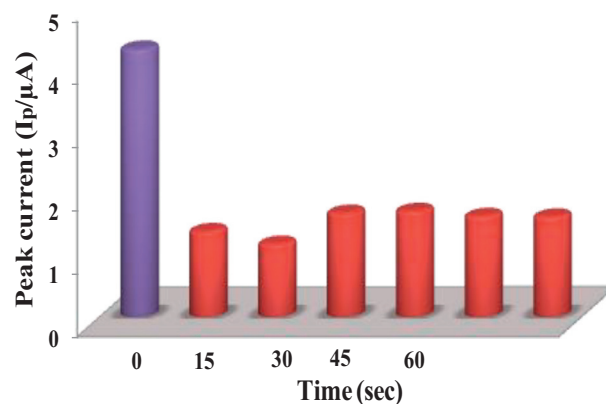


Fig. 4. Influence of time on the peak current.

The largest oxidation peak is observed for a pre-concentration time of 0 s (Fig. 4). This effect indicates that drenched adsorption on the modified sensor is achieved without accumulation time. Hence, further studies were carried out with no pre-concentration time.

### 3.6. Electrochemical behavior of MDH

The applicability of the ZnO-GCE for the electrochemical investigations of MDH was examined by using the CV technique (Fig. 5). The oxidation of MDH in PBS of pH 10.4 at the GCE and the modified GCE was also compared. No peaks were detected in the absence of MDH; where as in the presence of MDH, one well-resolved oxidation peak was observed. Therefore, the present reaction is an irreversible process. Furthermore, with the ZnO-GCE, the oxidation peak appeared at a slightly lesser potential and with a larger peak current compared to the bare GCE. This outcome mainly due to the modifier's highest electrocatalytic activity, which has not only increased the peak current but has also increased the sharpness of the oxidation peak. ZnO nanoparticles are effective in promoting the kinetics of electrochemical reaction. The results may be ascribed to the high conductivity, good antifouling property, fast electron transfer rate, and high electrochemical activity of the ZnO. Consequently, the subsequent oxidation peak current of MDH on the modified electrode increased greatly. The loading of ZnO nanoparticles increased the electrode surface area, which enabled more analyte to come in contact with the electrode surface to get

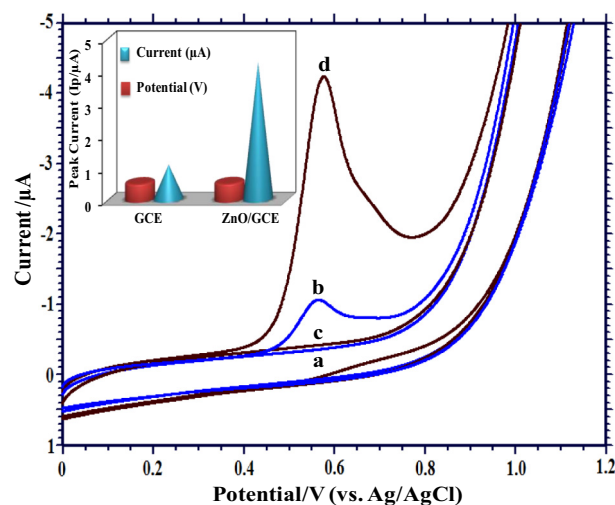


Fig. 5. Electrochemical behavior of 1.0 mM MDH in pH 10.4, at scan rate = 0.05  $\text{Vs}^{-1}$ ; (a) blank GCE; (b) CV of 1.0 mM MDH at GCE; (c) blank ZnO-GCE; (d) CV of 1.0 mM MDH at ZnO-GCE. Inset: Variation in peak current and peak potential at bare and modified GCE.

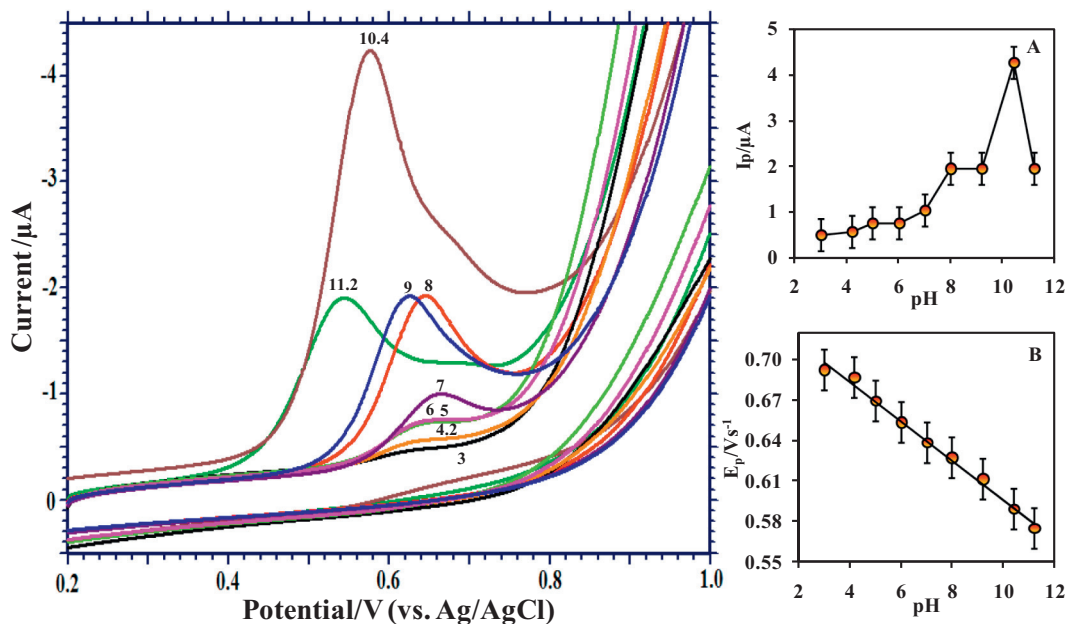


Fig. 6. Study of supporting electrolyte pH effect using CV technique at ZnO-GCE of 1.0 mM MDH; Scan rate = 0.05  $\text{Vs}^{-1}$ ; (A) Influence of pH on the peak potential  $E_p / \text{V}$ ; (B) Influence of pH on the peak current  $I_p / \mu\text{A}$ .

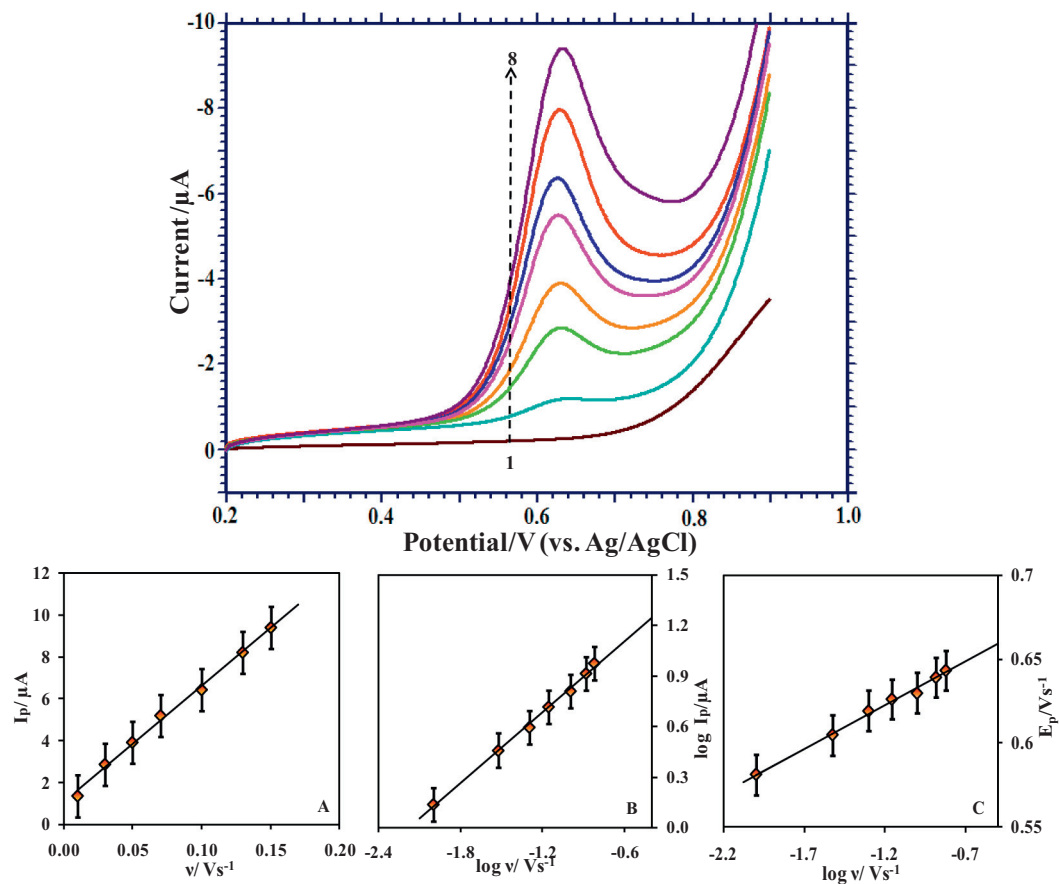


Fig. 7. Impact of sweep rate on 1.0 mM MDH in pH 10.4 at ZnO-GCE: (1) blank; (2) 0.01; (3) 0.03; (4) 0.05; (5) 0.07; (6) 0.1; (7) 0.13; (8) 0.15  $\text{Vs}^{-1}$ . (A) Plot of peak current ( $I_p / \mu\text{A}$ ) versus scan rate ( $v / \text{Vs}^{-1}$ ); (B) Plot of  $\log I_p / \mu\text{A}$  versus  $\log v / \text{Vs}^{-1}$ ; (C) Plot of variation of  $E_p / \text{V}$  versus  $\log v / \text{Vs}^{-1}$ .

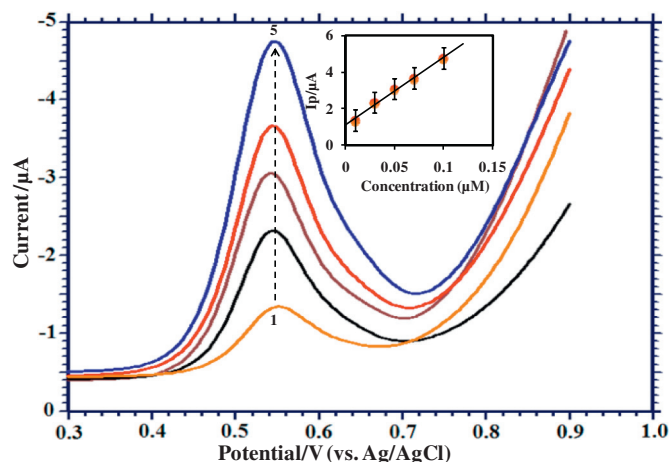


Fig. 8. Study of concentration variation of MDH using SWV technique at ZnO-GCE: (1) 0.01; (2) 0.03; (3) 0.05; (4) 0.07; (5) 0.1  $\mu\text{M}$ . Inset: Plot of concentration versus peak current  $I_p / \mu\text{A}$ .

Table 1  
Comparison of detection limits of MDH by various working electrodes.

Techniques and sensors utilized	LOD	Reference
Differential pulse voltammetry using GCE <sup>a</sup>	$0.1 \times 10^{-6}$	[24]
Square wave voltammetry using ZnO-GCE	$7.25 \times 10^{-8}$	[Present work]

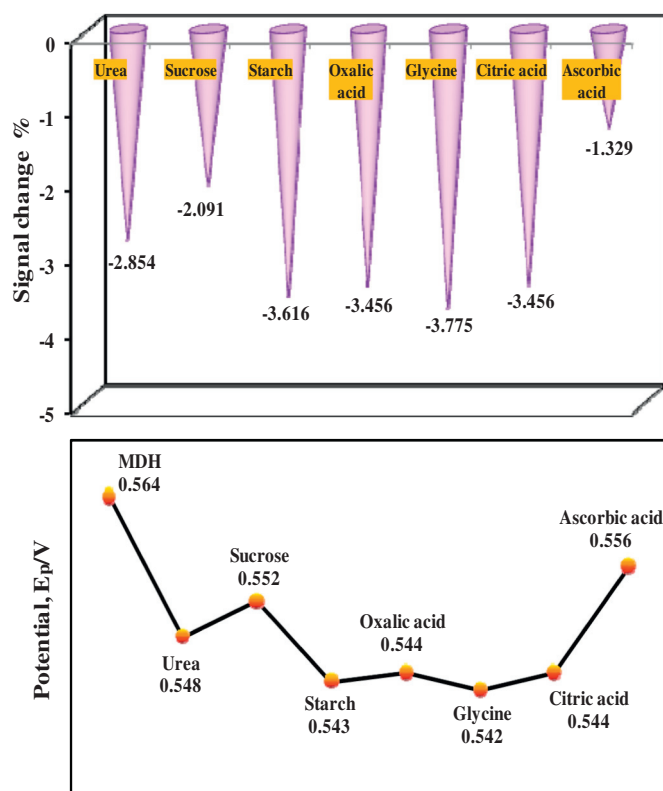


Fig. 9. Voltammetric behavior of MDH in presence of excipients.

oxidized. In addition, the modified electrode also enabled more efficient transfer of electrons [28–30].

### 3.7. Effect of supporting electrolyte

pH of the supporting electrolyte influences the rate of electron

Table 2  
Application of SWV for the determination of MDH in pharmaceutical samples and spiked human urine samples.

Pharmaceutical samples	Spiked ( $10^{-6}$ M)	Detected <sup>a</sup> ( $10^{-6}$ M)	Recovery
Sample 1	1.0	0.9861	98.61
Sample 2	5.0	4.7250	94.50
Sample 3	8.0	7.5978	94.97

Urine samples	Spiked ( $10^{-4}$ M)	Detected <sup>a</sup> ( $10^{-4}$ M)	RSD	% RSD
Sample 1	0.1	0.0984	0.01909	1.909
Sample 2	0.5	0.4745	0.01981	1.981
Sample 3	1.0	0.9786	0.19212	1.921

<sup>a</sup> Average five readings.

transfer and the electrochemical nature of MDH. Hence, the impact of pH variation of 0.2 M PBS in the range of 3.0–11.2 was examined using the CV technique (Fig. 6). Variations in the peak potentials and peak currents were observed as the pH of the solution was changed. Peak currents increased gradually till a pH of 10.4, and subsequently decreased with further increase in the pH due to the protonation of the analyte. Since a well-defined oxidation peak with maximum peak current is observed for a pH of 10.4 (Fig. 6A), that is considered optimal for further studies.

In addition, the peaks are shifted slightly towards negative potentials with increase in the pH, implying that the present electrode process involves protons (Fig. 6B) [29]. The value of the slope shows that an unequal number of protons and electrons are involved in the electrooxidation of MDH [24].

$$E_p = -0.014 \text{ pH} + 0.741; R^2 = 0.992$$

### 3.8. Influence of sweep rate

The LSV technique was used to study the impact of the sweep rate on the behavior of MDH at the ZnO-GCE for a pH of 10.4 (Fig. 7). From the study, we observe that, there is positive shift of potential with the enhancement of current for every increase in the scan rate (Fig. 7A). The enhancement in the peak current with increase in the sweep rate is ascribed to the excitation of signal caused during the charging of the interface capacitance by the charge transfer progression. In addition, a linear equation is obtained for the logarithm of peak current versus logarithm of scan rate (Fig. 7B) with corresponding regression equations as shown below:

$$\log I_p (\mu\text{A}) = 0.701 \log \nu + 1.528; R^2 = 0.996$$

The slope value showed that the electrode process was mixed adsorption diffusion controlled one. This process may be initiated with the adsorption of the drug moiety i.e. MDH at the sensing base, followed by their diffusion through the surface [31].

Furthermore, the relation between  $E_p$  and  $\log \nu$  is also found to be linear (Fig. 7C). This relation between  $\nu$  and  $E_p$  for a process involving sensors can be explained by Laviron's theory [32]:

$$E_p = E^0 + \left( \frac{2.303RT}{\alpha nF} \right) \log \left( \frac{RTk^0}{\alpha nF} \right) + \left( \frac{2.303RT}{\alpha nF} \right) \log \nu \quad (2)$$

Based on Bard and Faulkner transfer coefficient  $\alpha$  [33], the heterogeneous rate constant and the number of electrons were calculated.

$$\Delta E_p = E_p - E_{p/2} = \frac{47.7}{\alpha n} \text{ mV} \quad (3)$$

Here,  $E_{p/2}$  is the potential at which the current is equal to half the peak value. From this, we obtain the value of  $\alpha$  to be 0.55. From the intercept of  $E_p$  versus  $\log \nu$ ,  $k^0$  was calculated to be  $3.75 \times 10^3 \text{ s}^{-1}$ . Furthermore, the number of the electrons ( $n$ ) transferred in the

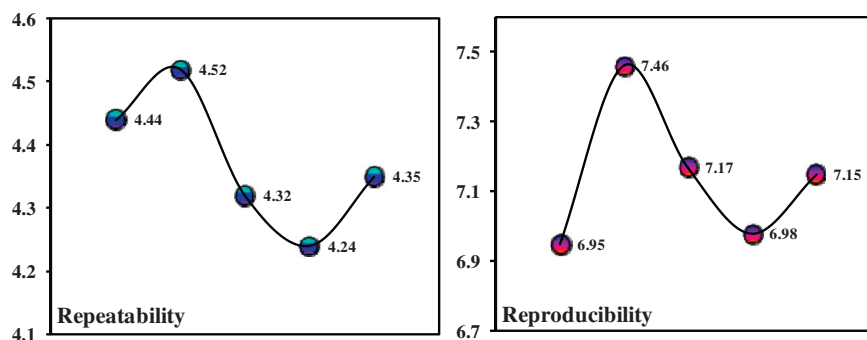


Fig. 10. Repeatability and reproducibility of the proposed sensor.

electrooxidation of MDH was calculated to be  $2.06 \approx 2$ .

## 4. Analytical applications

### 4.1. Concentration variation of MDH

The quantitative detection of MDH was performed by the SWV technique under optimal conditions at the ZnO-GCE. The peak current response lies in the concentration range of 0.01–0.1  $\mu\text{M}$  MDH at the fabricated sensor (Fig. 8).

The relevant equation is  $I_p (\mu\text{A}) = 37.02C (\mu\text{M}) + 1.102$ ;  $R^2 = 0.992$ . From the calculations, limit of detection (LOD =  $3S/M$ ) of  $7.25 \times 10^{-8} \text{M}$  and a limit of quantitation (LOQ =  $10S/M$ ) of  $2.42 \times 10^{-7} \text{M}$  was obtained ( $S$  = blank standard deviation,  $M$  = slope) [34–36]. The value of LOD observed in this SWV measurement was compared with the methods reported earlier. The low values of LOD and LOQ highlight the sensitivity of our method (Table 1).

### 4.2. Effect of excipients

To check the selectivity of the modified electrodes for MDH, the interference effect was examined using common interfering metabolites. The behavior of MDH was studied in the presence of excipients such as urea, sucrose, starch, oxalic acid, glycine, citric acid, and ascorbic acid. The results of the analysis are recorded in Fig. 9. It was noticed that several folds excess of these metabolites did not have any influence on the signal from a 1.0 mM MDH solution. Hence, the fabricated sensor can be utilized for the accurate and selective detection of MDH.

### 4.3. Detection of MDH in pharmaceutical samples and urine samples

The fabricated electrodes were used for the analysis of MDH in pharmaceutical products, to investigate the accuracy and reliability of the proposed method. As discussed in subsection 2.4, known quantities of standard MDH solutions were added to respective pre-analyzed tablet samples to examine the recovery. A high percentage recovery indicated that no interferents or additives affected the MDH analysis, and the resulting low RSD values highlighted the reproducibility of the method (Table 2).

The practical applicability of the prepared electrode was examined by analyzing MDH in fortified human urine samples, without any pre-treatment process. For this, drug-free urine samples were spiked with known amounts of MDH and analyzed as illustrated for syrup analysis. Good recoveries obtained for the tablet and spiked urine sample demonstrate that the projected method can be successfully applied for practical sample analysis (Table 2).

### 4.4. Repeatability and reproducibility of the ZnO-GCE

To study the repeatability of sensing tool, efficiency was checked for 20 days by preserving the prepared sensors in an airtight jar. The sensor maintained 98% of its initial peak response for a 1.0 mM MDH sample. This reveals the long shelf-life of the ZnO-GCE. At ambient temperature, the reproducibility of the sensor was explored via an intra-day study. Five measurements were documented by taking a stable concentration of MDH. A relative standard deviation (RSD) of about 2.5% was obtained for the sensor, showing good reproducibility for MDH detection (Fig. 10). The result shows that the fabricated electrodes have long-term stability and reproducibility, which is essential for analytical applications.

## 5. Conclusions

For the first time, ZnO nanoparticles were introduced as an efficient modifier on the surface of the GCE; thus, a sensing tool for the quantification of MDH was fabricated. ZnO showed many exceptional properties such as high electrical conductivity, sensitivity, reproducibility, mechanical strength, and a large surface area. The surface characteristics of the modifiers were studied by SEM, TEM, and XRD analyses. The CV, LSV, and SWV techniques were utilized to determine the various electrochemical parameters. Compared to the nascent GCE, the ZnO-GCE showed improved resolution and sensitivity with selectivity towards MDH at a pH of 10.4. An irreversible, mixed adsorption-diffusion controlled process was observed with the participation of an unequal number of protons and electrons. In contrast to earlier reports, the technique used in this study is very significant because of its impact, molecular selectivity, and high sensitivity reflected in the low LOD value. The validity of the current methodology was successfully established by the quantification of MDH in commercially available syrup. Furthermore, the versatility of the fabricated electrode was validated by the sensitive detection of MDH in human urine samples.

## References

- [1] S. Shahrokhian, L. Naderi, M. Ghalkhani, Mater. Sci. Eng., C 61 (2016) 842.
- [2] N.P. Shetti, D.S. Nayak, G.T. Kuchinad, R.R. Naik, Electrochim. Acta 269 (2018) 204.
- [3] V. Erady, R.J. Mascarenhas, A.K. Satpati, S. Detriche, Z. Mekhalif, J. Delhalle, A. Dhason, Mater. Sci. Eng. C Mater. Biol. Appl. 76 (2017) 114.
- [4] R. Jain, Vikas, Colloids Surf. B., 2011, 87, 423.
- [5] R.N. Goyal, D. Kaur, A.K. Pandey, Open Chem. Biomed. Methods J. 3 (2010) 115.
- [6] N.P. Shetti, D.S. Nayak, S.J. Malode, K.R. Reddy, S.S. Shukla, T.M. Aminabhavi, Colloids Surf. B Biointerfaces 177 (2019) 407.
- [7] N.P. Shetti, D.S. Nayak, S.J. Malode, R.M. Kulkarni, Sens. Bio-sensing Res. 14 (2017) 39.
- [8] H.T. Hsueh, S.J. Chang, F.Y. Hung, W.Y. Weng, C.L. Hsu, T.J. Hsueh, T.Y. Tsai, B.T. Dai, Super Lattices Microstruct. 49 (2011) 572.
- [9] M. Karimi, J. Saydi, M. Mahmoodi, J. Seidi, M. Ezzati, S. Shamsi Anari, B. Ghasemian, J. Phys. Chem. Solids 74 (2013) 1392.
- [10] Y. Li, B. Yao, R. Deng, B. Li, Z. Zhang, C. Shan, D. Zhao, D. Shen, J. Alloys Compd. 575 (2013) 233.
- [11] M.H. Koch, P.Y. Timbrell, R.N. Lamb, Semicond. Sci. Technol. 10 (1995) 1523.

- [12] M.R. Parra, P. Pandey, H. Siddiqui, V. Sudhakar, K. Krishnamoorthy, F.Z. Haque, *Appl. Surf. Sci.* 470 (2019) 1130.
- [13] S. Chaudhary, A. Umar, K.K. Bhasin, S. Baskoutas, *Materials* 11 (2018) 287.
- [14] N.P. Shetti, S.J. Malode, D. Ilager, K.R. Reddy, S.S. Shukla, T.M. Aminabhavi, *Electroanal.* 31 (2019) 1.
- [15] N.P. Shetti, D.S. Nayak, S.J. Malode, R.M. Kulkarni, D.B. Kulkarni, R.A. Teggi, V.V. Joshi, *Surf. Interfac.* 9 (2017) 107.
- [16] N.P. Shetti, S.J. Malode, S.T. Nandibewoor, *Bioelectrochem.* 88 (2012) 76.
- [17] M. Gordon (Ed.), *Psycho Pharmacological Agents*, 2 Academic Press, New York, 1994.
- [18] H.Y. Mohammed, F.F. Cantwell, *Anal. Chem.* 50 (1978) 491.
- [19] R.T. Sane, L.S. Joshi, R.M. Kothurkar, K.D. Ladage, R.V. Tendolkar, D.P. Gangal, *Indian J. Pharm. Sci.* 52 (1990) 160.
- [20] N.W. Smith, M.B. Evans, *Chromatographia* 41 (1995) 197.
- [21] C.S.P. Sastry, A.S.R. Prasad Tipirneni, M.V. Suryanarayana, T. Thirupathi Rao, T. Satyanarayana, *Indian J. Pharm. Sci.* 52 (1990) 115.
- [22] D.F. Gurka, R.E. Kolinski, J.W. Myrick, C.E. Wells, *J. Pharm. Sci.* 69 (1980) 1069.
- [23] J. Emmanuel, R. Mathew, *Indian Drugs* 22 (1985) 602.
- [24] N.P. Shetti, D.S. Nayak, S.D. Bukkitgar, *Cogent Chem.* 1153274 (2016) 1.
- [25] N.P. Shetti, D.S. Nayak, S.J. Malode, R.R. Kakarla, S.S. Shukla, T.M. Aminabhavi, *Anal. Chim. Acta* 1051 (2019) 58–72.
- [26] N.P. Shetti, S.J. Malode, R.S. Malladi, S.L. Nargund, S.S. Shukla, T.M. Aminabhavi, *Microchem. J.* 146 (2019) 387–392.
- [27] P.K. Kalambate, A.K. Srivastava, *Sensors Actuators B Chem.* 233 (2016) 237.
- [28] S.D. Bukkitgar, N.P. Shetti, R.M. Kulkarni, S.T. Nandibewoor, *RSC Adv.* 5 (2015) 104891.
- [29] B.S. Dakshayini, K.R. Reddy, A. Mishra, N.P. Shetti, S.J. Malode, S. Basu, S. Naveen, A.V. Raghunath, *Microchem. J.* 147 (2019) 7.
- [30] R. Jagadish, S. Yellappa, M. Mahanthappa, K.B. Chandrasekhar, *J. Chin. Chem. Soc.* 64 (2017) 813.
- [31] N.P. Shetti, D.S. Nayak, S.J. Malode, R.M. Kulkarni, *J. Electrochem. Soc.* 164 (2017) B3036.
- [32] E. Laviron, *J. Electroanal. Chem.* 101 (1979) 19.
- [33] A.J. Bard, L.R. Faulkner, *Electrochemical Methods: Fundamentals and Applications*, 2nd ed., John Wiley and Sons, New York, 2004.
- [34] M. Swartz, I. Krull, *Analytical Method Development and Validation*, Marcel Dekker, New York, 1997.
- [35] A.K. Bhakta, R.J. Mascarenhas, O.J. D'Souza, A.K. Satpati, S. Detriche, Z. Mekhalif, J. Dalhalla, *Mater. Sci. Eng. C* 57 (2015) 328.
- [36] M. Brycht, K. Kaczmarek, B. Uslu, S.A. Ozkan, S. Skrzypek, *Diam. Relat. Mater.* 68 (2016) 13.